RSC Advances

PAPER

View Article Online
View Journal | View Issue

Cite this: *RSC Adv.*, 2020, **10**, 2646

Synergic effect of doxorubicin release and two-photon irradiation of Mn^{2+}-doped Prussian blue nanoparticles on cancer therapy†

Lamiaa M. A. Ali,‡[ab] Emna Mathlouthi,‡[cd] Maëlle Cahu,[c] Saad Sene,[c] Morgane Daurat,[ae] Jérôme Long,[c] Yannick Guari,[c] Fabrice Salles,[c] Joël Chopineau,[c] Jean-Marie Devoisselle,[c] Joulia Larionova*[c] and Magali Gary-Bobo*[a]

Received 4th November 2019
Accepted 2nd January 2020

DOI: 10.1039/c9ra09133e

rsc.li/rsc-advances

We demonstrate here that Mn^{2+}-doped Prussian blue nanoparticles of *ca.* 55 nm loaded with doxorubicin may be used as efficient therapeutic agents for combined photothermal and chemo-therapy of cancer cells with a synergic effect under two photon irradiation.

Photothermal therapy (PTT) is a promising strategy for the therapeutic treatment of tumours, which consists in "burning" cancer cells by laser irradiation at low energy wavelengths in the presence of an NIR photo-adsorbing agent.[1,2] In comparison to conventional cancer treatments, it offers several advantages, such as high specificity, deep penetration, lower tumour recurrence, minimal invasiveness and low toxicity to normal tissues.[3,4] Due to the fact that the treatment efficiency highly depends on the outstanding capacity of the PTT agent to convert light into heat, numerous materials have recently been reported, such as organic dyes[5,6] or various inorganic nano-objects, including metallic nanostructures (Au nanorods or nanoshells, Ag, Pd), carbon based materials (nanotubes, spheres, graphene oxide), transition metal dichalcogenide nanoparticles, metal oxide nano-objects or up-conversion nanocrystals.[7–16]

Among these, Prussian blue (PB) nano-objects have been developed as interesting PTT agents since they benefit from many advantages, such as: (i) a controlled size ranging from a few to hundreds of nanometers, (ii) easy surface functionalization, (iii) excellent absorption properties in the NIR spectral domain due to an Fe^{2+} to Fe^{3+} intervalence charge transfer band ranging from 650 to 900 nm, (iv) high stability under irradiation, and (v) the fact that bulk PB is validated by the FDA under the brand name Radiogardase® as an antidote for human beings exposed to radioactive Cs^{+}.[17] It has been shown *in vitro* that PB nanoparticles upon single photon excitation (SPE) (at 808 nm) can convert the laser irradiation into thermal energy contributing to an important temperature increase.[18,19] Their efficiency depends on the nanoparticles' concentration, their chemical composition, the laser power, the mode of irradiation and the irradiation time. Moreover, it has been demonstrated that nano-sized PB presents a higher efficiency in comparison with Au nanorods and a better photothermal stability than organic dyes used as conventional photothermal agents.[19,20] PTT effect of PB nanoparticles has also been demonstrated *in vivo* through their intra-tumoral injection that causes significant tumour necrosis 24 h after NIR irradiation in comparison with non-treated mice.[18] Nevertheless, the complete eradication of cancer cells using solely PTT treatment is rather difficult due to the suboptimal laser energy in deep tissues related to light scattering and absorption effects, a limited light penetration and the insufficient tumour target specificity of PTT agents. Some of these drawbacks may be circumvented using two photon excitation (TPE), which permits to increase the penetration depth and laser focalization allowing selective and efficient destruction of the targeted cancer cells with less damage to healthy tissues.[21–23] In this line of thought, we reported recently Mn^{2+}-doped PB nanoparticles of *ca.* 70 nm as efficient multifunctional PTT agents permitting to eradicate 97% of cancer cells 24 h after irradiation under TPE during 10 min, which may also be followed by Magnetic Resonance Imaging (MRI).[24] However, the comparison between the efficiency of the single and two-photon excitations on the same nano-objects has never been investigated.

[a]*Institut des Biomolécules Max Mousseron, UMR5247, Université de Montpellier, CNRS, ENSCM, Faculté de Pharmacie, 15 Avenue Charles Flahault, 34093 Montpellier Cedex 05, France. E-mail: magali.gary-bobo@inserm.fr*

[b]*Department of Biochemistry, Medical Research Institute, University of Alexandria, Alexandria, Egypt*

[c]*Institut Charles Gerhardt, Université de Montpellier, CNRS, ENSCM, Place Eugène Bataillon, 34095 Montpellier Cedex 5, France. E-mail: joulia.larionova@umontpellier.fr*

[d]*Université de Tunis el Manar, Faculté des Sciences, UR/11/ES/19, Physico-chimie des matériaux à l'état condensé, 2092, Tunis, Tunisia*

[e]*NanoMedSyn, 15 Avenue Charles Flahault, 34093 Montpellier, France*

† Electronic supplementary information (ESI) available. See DOI: 10.1039/c9ra09133e

‡ These two authors contribute equally to the article.

Another possibility to increase treatment efficiency and thus decrease the concentration of the PTT agent consists in the association of PTT with a drug or gene delivery to develop a personalized cancer therapy.[25–29] Several works report on the design of PB nanoparticles wrapped by gelatine or PEGylated lipids containing the incorporated anticancer drug[1,25,30–32] or conjugated with pDNA[33] or antigen specific cytotoxic lymphocytes.[34] In these cases, an improvement in cancer cell mortality or in the efficiency of gene transfection under NIR irradiation has been observed. But the synergic effect of PTT and chemotherapy has been clearly demonstrated only for hollow PB nanoparticles of 236 nm loaded with DOX presenting a therapeutic efficacy increase from 13.6 to 51.2% in comparison with the non-loaded nanoparticles.[20]

Herein, we investigate the loading of Mn^{2+}-doped PB nanoparticles of *ca.* 55 nm with DOX by experimental means joined with a theoretical modelling and demonstrate that such systems may be used as efficient agents for combined PTT and chemotherapy, able to eradicate almost all cancer cells (91%) under TPE due to a synergic effect with a relatively low concentration (50 μg mL^{-1}). Moreover, we compare for the first time the efficiency of the nano-objects with TPE and SPE and investigate their cytotoxicity. The Mn^{2+} doped PB nanoparticles have been chosen for this study due to their multifunctionality as MRI contrast agents and PTT therapeutic agent, since the presence of Mn^{2+} ion in such amount does not impact the PTT efficiency.[24]

Mn^{2+}-doped PB nanoparticles $Na_{0.38}Mn_{0.12}Fe[Fe(CN)_6]_{0.91}$ **1** have been obtained by using the previously described procedure involving the controlled self-assembling reaction between $Na_4[Fe(CN)_6]\cdot 10H_2O$, $FeCl_3\cdot 6H_2O$ and $MnCl_2\cdot 6H_2O$ in water. The drug loading was performed by suspending **1** in an aqueous DOX solution for 24 h under stirring in the dark. The loading capacity of DOX of 7.6 wt% (ratio between the adsorbed DOX weight and the total weight of the loaded nanoparticles) was determined by UV-Vis absorption spectroscopy (see Experimental part and Fig. S1, ESI†). The obtained nanoparticles $Na_{0.28}Mn_{0.12}Fe[Fe(CN)_6]_{0.88}@DOX_{0.04}$ **1@DOX** present typical stretching vibrations of the bridging cyanide group $\nu(Fe^{II}–CN–Fe^{III})$ at 2080 cm^{-1} in the FTIR spectra, as the pristine nanoparticles **1** with an appearance of small intensity bands fingerprints of DOX in the 800–1500 cm^{-1} frequency range (Fig. S2, ESI†). Their Powder X-ray diffraction pattern shows the typical fcc structure with a lattice parameter $a = 10.0$ Å (Fig. S3, ESI†). The obtained zeta potential (negative value) of −20.8 mV is slightly lower than for the pristine nanoparticles **1** (zeta potential of −35.7 mV), that suggests a surface modification after DOX loading. Transmission Electronic Microscopy (TEM) images for **1@DOX** reveal typical cubic nanoparticles with a mean size of 55 ± 13 nm (Fig. 1a, S4 and S5, ESI†). A slight bathochromic shift from 725 to 757 nm can be observed in the absorption spectra for **1@DOX** in comparison with **1** (Fig. S6†). Yet, due to the relatively small quantity of the adsorbed DOX, its characteristic band at 480 nm is not visible on the spectra of nanoparticles (Fig. S6, ESI†).

In order to provide an insight about the nature of interactions between DOX and the PB network, Monte-Carlo calculations using classical force field have been performed (see ESI† for details[35–37]). The size of DOX molecules of 16 Å × 9 Å × 8 Å is clearly larger in comparison with the size of the classical pores of the PB network generated by the presence of both, tetrahedral sites and cyanometallates' monovacancies, except in the case of double lacunas, in which DOX molecules can be fixed (Fig. 1b, S7, ESI†). The results of the Monte-Carlo simulations indicate that the saturation of doxorubicin molecules inside the pores is equal to 5.0 wt% (related to 7.6 wt% found experimentally). The larger experimental loading suggests that DOX is situated within the pores of the network (accessible double lacunas) and also at the surface of the nanoparticles attached by physisorption, as suggested by the change in the zeta potential. But the presence of covalent bonds between the nanoparticles and amino and OH groups cannot be excluded.

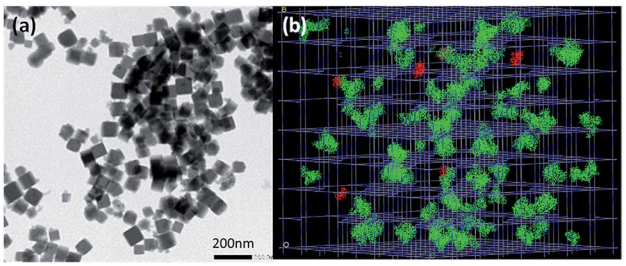

Fig. 1 (a) TEM image for **1@DOX**; (b) snapshot illustrating the PB network and the density of DOX inside from Monte Carlo simulations (red points = density of DOX presence; green points = density of presence of Na^+).

The DOX release experiments performed for **1@DOX** in phosphate buffered saline (PBS) show a slow and quasi-linear drug release during the first 4 hours and a more gradual behaviour resulting in a 10.3% release of the adsorbed DOX after 48 h (Fig. S8†).

In order to evaluate the safety of the nanoparticles, an *in vitro* cytotoxicity study has been carried out on human breast adenocarcinoma MDA-MB-231 cell line, which is treated with nanoparticles **1** and **1@DOX** at a concentration of 50 μg mL^{-1} and cell viability was determined after 1, 2 and 3 days. Results showed that **1** are non-toxic, as indicated by the increase of the percentage of cell viability with time, a similar behaviour as for untreated cells, which suggests their biocompatibility (Fig. S9, ESI†).[1,38,39] In contrast, cell death was observed in cells treated with **1@DOX**, where cell viability decreases during the treatment (40% after 1 day, 35% after 2 days, and 32% after 3 days) due to DOX release.

Chemo-PTT ability of the nanoparticles **1@DOX** to kill the living cancer MDA-MB-231 cells has been investigated by using both, TPE and SPE lasers and compared with the efficiency of nanoparticles **1** and free DOX at a concentration of 6 mg mL^{-1}. The latter is comparable with the amount of loaded DOX into nanoparticles **1@DOX**.

In the case of pulsed TPE at 808 nm (3.7 W, 5% of total laser power) for 10 min and after 24 h of irradiation, the cells treated with 50 μg mL^{-1} of **1@DOX** show 91 ± 7% of cell death, while it was 76 ± 12% in the case of **1** and 24 ± 17% for cells treated

with free DOX (Fig. 2a). These results were analysed by using CompuSyn software (ComboSyn, Inc)[40] in order to determine the synergic effect of combined PTT and drug. The calculated combination index (CI) value of 0.4 confirms the presence of an important synergistic effect (the synergic effect is operational for CI value lower than 1, while the additive and antagonist effects occur for values equal or greater than 1, respectively). The cell death is highlighted by confocal imaging on green fluorescent living cells as shown in Fig. 2b. The safety of TPE laser was confirmed on untreated cells by the increase in the number of green fluorescent spots signifying their important multiplication 24 h after irradiation. On the contrary, a decrease or an almost completely disappearance of green fluorescent nuclei was observed 24 h after irradiation in cells treated with free DOX, **1** or **1@DOX**, confirming cell death. The synergic effect is certainly due to the important temperature elevation around each nanoparticle permitting the efficient DOX liberation.

The increase of nanoparticles concentration to 100 μg mL^{-1} did not hardly impact the efficiency of the treatment. In fact, 95 ± 4%, 89 ± 6% and 34 ± 1% of cell death were found for **1@DOX**, **1** and free DOX, respectively. This fact may be explained by the restricted amount of nanoparticles uptake at higher concentration. The effect of the concentration of **1@DOX** on cells mortality is shown on Fig. S10.†

The obtained results with the TPE laser have been compared with the effect obtained under the SPE laser by using the same concentration of nanoparticles. For this, cells were irradiated at 808 nm (2.5 W cm^{-2}) during 30 min (10 min of irradiation did not provide any cells' mortality). Data showed that only 35 ± 5% of cell death was found with **1@DOX** 24 h after irradiation (Fig. 3 and Fig. S11†) clearly demonstrating the advantage of TPE over SPE in our experimental conditions. However, the cancer cells continue to die and reached a death level of 55 ± 10% and 77 ± 3% after 48 h and 72 h of irradiation, respectively (Fig. 3a). Fluorescent images for live (green colour) and dead cells (red colour due to propidium iodide staining) confirm this result (Fig. 3b and S12†). Note that the obtained results on SPE are comparable with the previously published ones on other PB nanoparticles containing doxorubicin.[1,25,30,32]

In summary, we demonstrated that Mn^{2+}-doped PB nanoparticles of *ca.* 55 nm can be easily loaded with doxorubicin drug (7.6 wt%). We established for the first time by using theoretical modelling that the latter mainly enters into the network's pores and a minor amount is also attached on the surface of the nanoparticles. A synergic effect of the PTT and DOX release is observed upon the treatment of MDA-MB-231 cancer cells with a relatively low concentration of nanoparticles (50 μg mL^{-1}) under TPE laser inducing their almost total eradication. These results are much improved in comparison to the ones obtained by combined DOX release and PTT under an SPE laser taking the same concentration of nanoparticles, which provides lower cell mortality even 72 h

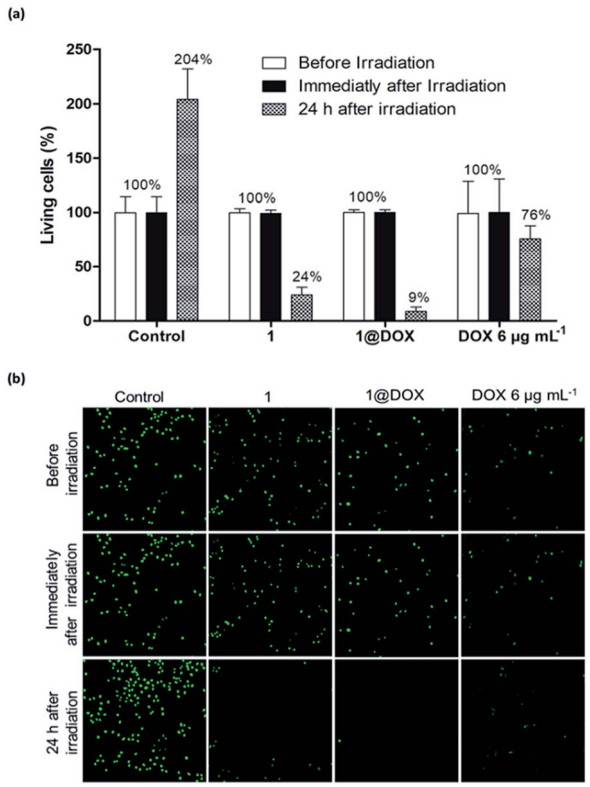

Fig. 2 (a) Cell counting (%) of living MDA-MB-231 cells treated with nanoparticles **1@DOX** and **1** at 50 μg mL^{-1} concentration and free doxorubicin before irradiation, immediately after irradiation and 24 h after irradiation with a TPE laser at 808 nm (3.7 W, 5% of total laser power) for 10 min. Data are presented as (mean ± SEM), $n = 3$. (b) Fluorescence imaging of living MDA-MB-231 cells treated with 50 μg mL^{-1} concentration of **1**, **1@DOX** and free doxorubicin (6 mg mL^{-1}) before irradiation, immediately and 24 h after irradiation with TPE laser at 808 nm (3.7 W, 5% of total laser power) for 10 min.

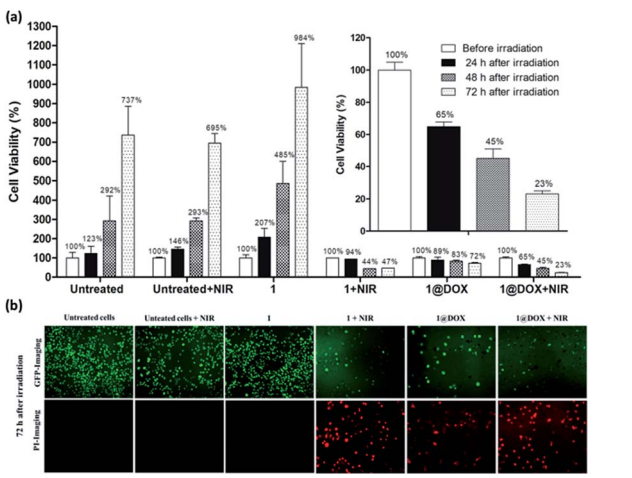

Fig. 3 (a) Cell counting (%) of living MDA-MB-231 cells treated with nanoparticles **1@DOX** and **1** at 50 μg mL^{-1} concentration before irradiation and 24 h, 48 h, and 72 h after irradiation with SPE laser at 808 nm (2.5 W cm^{-2}) for 30 min. Data are presented as (mean ± SEM) $n = 3$. Inset: enlargement of figure for **1@DOX** + NIR; (b) fluorescence imaging of living MDA-MB-231 cells treated with 50 μg mL^{-1} nanoparticles' concentration after 72 h of irradiation with SPE at 808 nm (2.5 W cm^{-2}) for 30 min. Cells were treated with propidium iodide (PI) for cell death detection (shown in red).

after irradiation. This strategy provides an interesting opportunity towards multifunctional nanomedicines with combined therapy and imaging.

Conflicts of interest

There are no conflicts to declare.

Acknowledgements

The authors thank the University of Montpellier and CNRS for financial support and PAC of ICGM for measurements. EM thanks the University Tunis el Manar for financial support. This work has been supported by ANR with grant number ANR-18-CE09-0012-01.

Notes and references

1 M. Wu, Q. Wang, X. Liu and J. Liu, *RSC Adv.*, 2015, **5**, 30970.
2 J. R. Melamed, R. S. Edelstein and E. S. Day, *ACS Nano*, 2015, **9**, 6.
3 L. Guo, W. Liu, G. Niu, P. Zhang, X. Zheng, Q. Jia, H. Zhang, J. Ge and P. Wang, *J. Mater. Chem. B*, 2017, **5**, 2832.
4 P. Xue, L. Sun, Q. Li, L. Zhang, Z. Xu, C. M. Li and Y. Kang, *J. Colloid Interface Sci.*, 2018, **509**, 384.
5 S. Luo, E. Zhang, Y. Su, T. Cheng and C. Shi, *Biomaterials*, 2011, **32**, 7127.
6 J. Pauli, T. Vag, R. Haag, M. Spieles, M. Wenzel, W. A. Kaiser, U. Resch-Genger and I. Hilger, *Eur. J. Med. Chem.*, 2009, **44**, 3496.
7 H. Norouzi, K. Khoshgard and F. Akbarzadeh, *Lasers Med. Sci.*, 2018, **33**, 917.
8 H. Shi, R. Yan, L. Wu, Y. Sun, S. Liu, Z. Zhou, J. He and D. Ye, *Acta Biomater.*, 2018, **72**, 256.
9 Z. Sobhani, M. A. Behnam, F. Emami, A. Dehghanian and I. Jamhiri, *Int. J. Nanomed.*, 2017, **12**, 4509.
10 J. Zhang, J. Chen, J. Ren, W. Guo, X. Li, R. Chen, J. Chelora, X. Cui, Y. Wan, X. J. Liang, Y. Hao and C. S. Lee, *Biomaterials*, 2018, **181**, 92.
11 M. Pérez-Hernández, P. Del Pino, S. G. Mitchell, M. Moros, G. Stepien, B. Pelaz, W. J. Parak, E. M. Gálvez, J. Pardo and J. M. de la Fuente, *ACS Nano*, 2015, **9**, 52.
12 Z. Zhou, Y. Wang, Y. Yan, Q. Zhang and Y. Cheng, *ACS Nano*, 2016, **10**, 4863.
13 X. Jiang, S. Zhang, F. Ren, L. Chen, J. Zeng, M. Zhu, Z. Cheng, M. Gao and Z. Li, *ACS Nano*, 2017, **11**, 5633.
14 R. Ghosh Chaudhuri and S. Paria, *Chem. Rev.*, 2012, **112**, 2373.
15 Y. Liu, K. Ai, J. Liu, M. Deng, Y. He and L. Lu, *Adv. Mater.*, 2013, **25**, 1353.
16 J. You, P. Zhang, F. Hu, Y. Du, H. Yuan, J. Zhu, Z. Wang, J. Zhou and C. Li, *Pharm. Res.*, 2014, **31**, 554.
17 J. Long, Y. Guari, C. Guérin and J. Larionova, *Dalton Trans.*, 2016, **45**, 17581.
18 H. A. Hoffman, L. Chakrabarti, M. F. Dumont, A. D. Sandler and R. Fernandes, *RSC Adv.*, 2014, **4**, 29729.
19 G. Fu, W. Liu, S. Feng and X. Yue, *Chem. Commun.*, 2012, **48**, 11567.
20 X. Cai, X. Jia, W. Gao, K. Zhang, M. Ma, S. Wang, Y. Zheng, J. Shi and H. Chen, *Adv. Funct. Mater.*, 2015, **25**, 2520.
21 J. L. Li, D. Day and M. Gu, *Adv. Mater.*, 2008, **20**, 3866.
22 J. Kim, S. Park, J. E. Lee, S. M. Jin, J. H. Lee, I. S. Lee, I. Yang, J. S. Kim, S. K. Kim, M. H. Cho and T. Hyeon, *Angew. Chem., Int. Ed. Engl.*, 2006, **45**, 7754.
23 S. M. Ardekani, A. Dehghani, M. Hassan, M. Kianinia, I. Aharonovich and V. G. Gomes, *Chem. Eng. J.*, 2017, **330**, 651.
24 L. M. A. Ali, E. Mathlouthi, M. Kajdan, M. Daurat, J. Long, R. Sidi-Boulenouar, M. Cardoso, C. Goze-Bac, N. Amdouni, Y. Guari, J. Larionova and M. Gary-Bobo, *Photodiagn. Photodyn. Ther.*, 2018, **22**, 65.
25 L. Zou, H. Wang, B. He, L. Zeng, T. Tan, H. Cao, X. He, Z. Zhang, S. Guo and Y. Li, *Theranostics*, 2016, **6**, 762.
26 Z. Zhang, J. Wang and C. Chen, *Adv. Mater.*, 2013, **25**, 3869.
27 Z. Xiao, C. Ji, J. Shi, E. M. Pridgen, J. Frieder, J. Wu and O. C. Farokhzad, *Angew. Chem., Int. Ed. Engl.*, 2012, **51**, 11853.
28 T. S. Hauck, T. L. Jennings, T. Yatsenko, J. C. Kumaradas and W. C. W. Chan, *Adv. Mater.*, 2008, **20**, 3832.
29 J. P. May and S.-D. Li, *Expert Opin. Drug Delivery*, 2013, **10**, 511.
30 P. Xue, K. K. Y. Cheong, Y. Wu and Y. Kang, *Colloids Surf., B*, 2015, **125**, 277.
31 L. Jing, S. Shao, Y. Wang, Y. Yang, X. Yue and Z. Dai, *Theranostics*, 2016, **6**, 40.
32 H. Chen, Y. Ma, X. Wang, X. Wu and Z. Zha, *RSC Adv.*, 2016, **7**, 248.
33 X.-D. Li, X. L. Liang, F. Ma, L. J. Jing, L. Lin, Y. B. Yang, S. S. Feng, G. L. Fu, X. L. Yue and Z. F. Dai, *Colloids Surf., B*, 2014, **123**, 629.
34 R. A. Burga, S. Patel, C. M. Bollard, C. R. Y Cruz and R. Fernandes, *Nanomedicine*, 2016, **11**, 1759.
35 X. Unamuno, E. Imbuluzqueta, F. Salles, P. Horcajada and M. J. Blanco-Prieto, *Eur. J. Pharm. Biopharm.*, 2018, **132**, 11.
36 S. Rojas, I. Colinet, D. Cunha, T. Hidalgo, F. Salles, C. Serre, N. Guillou and P. Horcajada, *ACS Omega*, 2018, **3**, 2994.
37 S. M. F. Vilela, P. Salcedo-Abraira, I. Colinet, F. Salles, M. C. de Koning, M. J. A. Joosen, C. Serre and P. Horcajada, *Nanomaterials*, 2017, **7**, 321.
38 G. Fu, W. Liu, Y. Li, Y. Jin, L. Jiang, X. Liang, S. Feng and Z. Dai, *Bioconjugate Chem.*, 2014, **25**, 1655.
39 W. Chen, K. Zeng, H. Liu, J. Ouyang, L. Wang, Y. Liu, H. Wang, L. Deng and Y.-N. Liu, *Adv. Funct. Mater.*, 2017, **27**, 1605795.
40 T.-C. Chou, *Pharmacol. Rev.*, 2006, **58**, 621.